low-energy active ions are not known. Our detected nitrogen therefore must be a measure of the degree to which process 3 occurs.

We suggest that once the N atoms come to rest in the bulk, the thermodynamic driving force for chemical reaction will be given by the free energy, ΔG, of the reaction involved. The free energies of formation of the metal nitrides are not all available, however, in cases where they are available it is found that they are similar to the enthalapies of formation. We can formulate idealized reactions of the type

$$\begin{matrix} \mathrm{Ti} & + & \mathrm{N} & \rightarrow & \mathrm{TiN} \\ 113 & & -67.5 & & \end{matrix} \qquad \Delta H^\circ = -180.5 \text{ kcal} \qquad (9)$$

The enthalapies of formation, ΔH°_f, for the reactants and products are indicated below the respective compounds and ΔH° for the reaction is shown on the right. It is obvious that reactions such as that of eq 9 can be written for the other metal nitrides and that the ΔH° values will become less negative as ΔH°_f of the nitride compound becomes less negative. The stoichiometries of our products may be different from those expressed by eq 9 and our reactants and products are not in their standard states. Despite these uncertainties, the ΔH° values do qualitatively follow the N/M intensity ratios of Table I. This relationship between ΔH° and the N/M intensity indicates that chemical reactions are taking place between the beam and surface; purely physical effects cannot explain the observed intensity ratios.

Conclusions

It has been shown that N_2^+ can be used to induce chemical reactions between N atoms and first-row transition metals. The reaction produces nitride layers at the surface that exhibit XPS spectra and thermal stabilities which are identical with those of pure metal nitrides. The nitrogen/metal ratio in the reacted layer can be correlated with the enthalapy of formation of the metal nitride. The selectivity and specificity of these beam–surface reactions suggests the use of such techniques for preparing surfaces with unique properties. The advantage of this *reactive ion bombardment* over conventional implantation is the ability to alter the chemical nature of a surface.

Acknowledgment. Acknowledgment is made to the U.S. Army Office of Research for support of this research.

References and Notes

(1) J. A. Taylor, G. M. Lancaster, A. Ignatiev, and J. W. Rabalais, *J. Chem. Phys.*, **68**, 1776 (1978).
(2) J. A. Taylor, G. M. Lancaster, and J. W. Rabalais, *J. Electron Spectrosc.*, **13**, 435 (1978).
(3) J. A. Taylor, G. M. Lancaster, and J. W. Rabalais, *J. Am. Chem. Soc.*, **100**, 4441 (1978).
(4) V. Franchetti, B. H. Solka, W. E. Baitinger, J. W. Amy, and R. G. Cooks, *Int. J. Mass Spectrom. Ion Phys.*, **23**, 29 (1977).
(5) A. Shepard, R. W. Hewitt, G. J. Slusser, W. E. Baitinger, R. G. Cooks, N. Winograd, W. N. Delgass, A. Varon, and G. Devant, *Chem. Phys. Lett.*, **44**, 371 (1976).
(6) K. S. Kim and N. Winograd, *Surface Sci.*, **43**, 625 (1974).
(7) K. S. Kim, W. E. Baitinger, J. W. Amy, and N. Winograd, *J. Electron Spectrosc.*, **5**, 351 (1974).
(8) K. S. Kim, W. E. Baitinger, and N. Winograd, *Surface Sci.*, **55**, 285 (1976).
(9) T. H. Lee, R. J. Colton, M. G. White, and J. W. Rabalais, *J. Am. Chem. Soc.*, **97**, 4845 (1975).
(10) J. H. Scofield, *J. Electron Spectrosc.*, **8**, 129 (1976).
(11) H. D. Hagstrum, *Phys. Rev.*, **122**, 83 (1961); **150**, 495 (1966); *Surface Sci.*, **54**, 197 (1976).
(12) H. F. Winters, *J. Appl. Phys.*, **43**, 4809 (1972); H. F. Winters and P. Sigmund, *Ibid.*, **45**, 4760 (1974); H. F. Winters and D. E. Horne, *Surface Sci.*, **24**, 587 (1971).
(13) The projected range is defined as the mean penetration depth for ions traveling normal to the surface.
(14) P. D. Townsend, J. C. Kelly, and N. E. W. Hartley, "Ion Implantation, Sputtering, and Their Applications", Academic Press, New York, 1976.
(15) P. H. Citrin and D. R. Hamann, *Chem. Phys. Lett.*, **22**, 301 (1973).

Detailed Calculations Modeling the Oscillatory Bray–Liebhafsky Reaction

David Edelson*

Bell Laboratories, Murray Hill, New Jersey 07974

and Richard M. Noyes

Department of Chemistry, University of Oregon, Eugene, Oregon 97403 *(Received September 11, 1978)*

Publication costs assisted by Bell Laboratories

The Bray–Liebhafsky reaction exhibits oscillations in the concentrations of iodine, iodide, and other species during the iodate-catalyzed decomposition of acidic hydrogen peroxide. We have assigned rate constants to a previously proposed mechanism and have reproduced the major features of experimental observations. The calculations are critically dependent upon the modeling of release of supersaturation by dissolved oxygen; we could not generate more than a few strongly damped oscillations unless we built replenishment of hydrogen peroxide into the model. The mechanism as developed uses only well known types of chemical species and elementary processes and is consistent with known rate constants and free energies of formation. Because we have reproduced such complicated behavior in spite of these severe restrictions, we believe the essential features of the proposed mechanism are strongly supported.

1. Introduction

One of the first known chemical oscillators was discovered by Bray[1] while examining the iodate-catalyzed decomposition of hydrogen peroxide. It was subsequently studied by Liebhafsky[2] at various times during a period of more than 40 years. Further study by Sharma and Noyes[3,4] led to a detailed mechanism described in a paper[4] which also provides a bibliography of previous work on the subject.

Our arguments for that mechanism were essentially qualitative, although Clarke[5] subsequently assured us the mechanism was of a form that could generate an unstable steady state for certain values of rate constants. Following our success with modeling the principal features of the

0022-3654/79/2083-0212$01.00/0

TABLE I

no.	reaction	rate constant[a]
A1	$HOI + I^- + H^+ \rightleftarrows I_2 + H_2O$	$4.30 \times 10^{12}\ M^{-2}\ s^{-1}$ $3.22 \times 10^{-1}\ M^{-1}\ s^{-1}$
A2	$HOIO + I^- + H^+ \rightleftarrows 2\ HOI$	$1.00 \times 10^{10}\ M^{-2}\ s^{-1}$ $7.65 \times 10^{-2}\ M^{-1}\ s^{-1}$
A3	$IO_3^- + I^- + 2\ H^+ \rightleftarrows HOIO + HOI$	$3.71 \times 10^{3}\ M^{-3}\ s^{-1}$ $2.27 \times 10^{5}\ M^{-1}\ s^{-1}$
A4	$2\ HOIO \rightleftarrows IO_3^- + HOI + H^+$	$5.56 \times 10^{7}\ M^{-1}\ s^{-1}$ $6.93 \times 10^{-6}\ M^{-2}\ s^{-1}$
B0	$HOI + HOOH \rightleftarrows I^- + O_2(aq) + H^+ + H_2O$	$1.08 \times 10^{2}\ M^{-1}\ s^{-1}$ $6.46 \times 10^{-8}\ M^{-3}\ s^{-1}$
B1	$HOIO + HOOH \rightleftarrows HOI + O_2(aq) + H_2O$	$1.70 \times 10^{1}\ M^{-1}\ s^{-1}$ $7.76 \times 10^{-20}\ M^{-2}\ s^{-1}$
B2	$IO_3^- + HOOH + H^+ \rightleftarrows HOIO + O_2(aq) + H_2O$	$3.01 \times 10^{-4}\ M^{-2}\ s^{-1}$ $1.10 \times 10^{-11}\ M^{-2}\ s^{-1}$
D1	$\cdot IO + HOOH \rightleftarrows HOIO + HO\cdot$	$1.00 \times 10^{7}\ M^{-1}\ s^{-1}$ $6.14 \times 10^{3}\ M^{-1}\ s^{-1}$
D2	$\cdot IO_2 + HOOH \rightleftarrows IO_3^- + H^+ + HO\cdot$	$1.00 \times 10^{4}\ M^{-1}\ s^{-1}$ $1.03 \times 10^{6}\ M^{-2}\ s^{-1}$
–Fi	$HOO\cdot + I_2 \rightleftarrows I^- + O_2(aq) + H^+ + \cdot I$	$1.69 \times 10^{6}\ M^{-1}\ s^{-1}$ $3.28 \times 10^{8}\ M^{-3}\ s^{-1}$
H1	$HO\cdot + HOOH \rightleftarrows H_2O + HOO\cdot$	$6.00 \times 10^{7}\ M^{-1}\ s^{-1}$ $7.33 \times 10^{-19}\ M^{-1}\ s^{-1}$
K0	$\cdot I + O_2(aq) \rightleftarrows \cdot OOI$	$1.00 \times 10^{8}\ M^{-1}\ s^{-1}$ $9.30 \times 10^{3}\ s^{-1}$
L0	$\cdot OOI + I^- + H^+ \rightleftarrows HOI + \cdot IO$	$1.40 \times 10^{10}/mM^{-2}\ s^{-1}$ $1.70 \times 10^{10}/mM^{-1}\ s^{-1}$
N2	$IO_3^- + HOIO + H^+ \rightleftarrows 2\cdot IO_2 + H_2O$	$1.06 \times 10^{3}\ M^{-2}\ s^{-1}$ $4.64 \times 10^{4}\ M^{-2}\ s^{-1}$
O1	$2\ HOO\cdot \rightleftarrows HOOH + O_2(aq)$	$1.00 \times 10^{6}\ M^{-1}\ s^{-1}$ $5.29 \times 10^{-16}\ M^{-1}\ s^{-1}$
O2	$\cdot I + HOO\cdot \rightleftarrows I^- + O_2(aq) + H^+$	$2.00 \times 10^{8}\ M^{-1}\ s^{-1}$ $3.36 \times 10^{-11}\ M^{-2}\ s^{-1}$
O3	$2\cdot I \rightleftarrows I_2$	$1.00 \times 10^{10}\ M^{-1}\ s^{-1}$ $1.74 \times 10^{-11}\ s^{-1}$
P	$O_2(aq) \rightleftarrows O_2(g)$	see text

[a] First value is for the forward reaction, the second for the reverse reaction where applicable.

oscillatory Belousov–Zhabotinsky reaction,[6,7] we initiated the present search to generate a self-consistent set of rate constants that would reproduce experimental observations of the Bray–Liebhafsky reaction.

The Bray–Liebhafsky reaction does not have any of the organic species whose radical oxidations generate much of the complexity of the Belousov–Zhabotinsky reaction,[7] and we anticipated the present undertaking would be somewhat simpler. We encountered other complexities associated with the difficulty of properly modeling the evolution of a reactive product gas from a supersaturated solution, but obtained results that strongly support our proposed mechanism. The argument is developed here in some detail to illustrate how attention to thermodynamic and other restrictions can reduce to manageable proportions what would otherwise be an excessive number of potentially significant items.

2. Model Mechanism

The mechanism finally adopted for the computations is presented in Table I. This was made up of reactions selected from the complete set,[4] the arguments for which have been previously published. Numbering of individual steps is the same as that used in the full mechanism. Reasons for selecting the steps in Table I can be summarized briefly as follows:

Steps A1–A4 are the only permissible oxyiodine processes involving the free element and species containing only one iodine atom providing all reactants and products have even numbers of electrons.

Steps B0–B2 are the only ways by which hydrogen peroxide can be oxidized by nonradical two-equivalent processes. They presumably involve peroxyacid intermediates that undergo electronic transitions to generate elementary oxygen. Rate constants selected are such that step B1 does not contribute significantly during most times of interest.

Steps in which hydrogen peroxide is reduced by two-equivalent processes (C steps) are thermodynamically allowed but too slow to be significant.

Steps D1 and D2 involve one-equivalent reduction of hydrogen peroxide by iodine containing radicals. The analogous reaction of iodine atoms is not included because the sequence (K0) + (L0) removes them more rapidly than hydrogen peroxide would.

Steps in which hydrogen peroxide is oxidized one equivalent by iodine containing radicals (E steps) are thermodynamically forbidden for $\cdot IO_2$ and $\cdot I$, while $\cdot IO$ apparently reacts preferentially by (D1).

Step –Fi is the most probable way for $HOO\cdot$ to be oxidized by a species with an even number of electrons; it may really be a simple electron transfer.

Step H1 will overwhelm all other plausible reactions of $HO\cdot$ (G steps).

Other reactions of iodine radicals (I, J, and M steps) are unimportant except for the peroxidation and reduction sequence (K0) + (L0). Therefore, the sequence (H1) + (–Fi) + (K0) + (L0) + (D1) represents a chain in which each radical has one and only one fate and in which the final step regenerates the radical necessary for the first step.

Step N2 represents the formation of radical species from those with even numbers of electrons. It is followed by (D2) to form $HO\cdot$ radicals and initiate the chain sequence mentioned above.

Steps O1–O3 are the only chain-terminating steps we have included. We argued previously[8] that $\cdot OOI$ radicals were rather sluggish to termination reactions, and the

radicals ·IO, ·IO_2, and HO· are rapidly scavenged by hydrogen peroxide. The rate constants finally adopted make step O3 the only terminating reaction of importance.

Step P is the relief of supersaturation by dissolved oxygen.

3. Qualitative Explanation of Mechanism

The previous section explains why various individual steps were accepted or rejected but does not explain why oscillations should result. The explanation developed in this section recognizes that the only stoichiometrically significant species are H_2O, HOOH, H^+, IO_3^-, I_2, and O_2. Although many other species are essential to the mechanism, they never attain concentrations significant compared to those listed and need not be included in equations describing net chemical change in the system.

The mechanism resembles that of other chemical oscillators[9] in that periods of reaction by nonradical processes generate conditions such that the system switches rapidly and autocatalytically to dominance by radical processes.

The nonradical period can only involve steps of types A, B, and P from Table I. Dominance by such steps occurs when the concentration of I^- is moderately high. Hydrogen peroxide is oxidized to oxygen and iodate is reduced to iodine by the net stoichiometry of process I.

$$2IO_3^- + 5HOOH + 2H^+ \rightarrow I_2 + 5O_2(g) + 6H_2O \quad (I)$$

It was argued previously[8] that the largest contribution to the stoichiometry of (I) results from the sequence 2(A3) + 2(A2) + 5(B0) + (A1) + 5(P). The computations reported here maintain iodide at such low concentrations at all times that the sequence 2(B2) + 2(A2) + 3(B0) + (A1) + 5(P) makes at least as large a contribution to nonradical process I. Steps A3 and B2 are rate determining for these parallel sequences while step A2 consumes HOIO much faster than do either (B1) or (A4).

Even when most of the reaction is nonradical, a few radicals are always being formed by step N2. For the steps and rate constants in Table I, radicals are destroyed almost entirely by step O3. Formation and destruction of radicals involves the sequence (N2) + 2(D2) + 2(H1) + 2(–Fi) + (O3) which generates the net stoichiometry of (II).

$$HOIO + 4HOOH + I_2 \rightarrow IO_3^- + 2O_2(aq) + 2I^- + 3H^+ + 3H_2O \quad (II)$$

Note that formation and destruction of radicals causes no net change in the average oxidation number of iodine species, but it does induce the disproportionation of hydrogen peroxide. The free energy change of that disproportionation makes process II thermodynamically favored even though the oxidation of HOIO by I_2 is not favored. Because a few radicals are always being formed and destroyed, the ratio of O_2 to I_2 produced will always be greater than the 5:1 predicted by the stoichiometry of process I, but the difference is relatively insignificant as long as nonradical processes are dominant.

If the concentration of dissolved oxygen is not too great, radicals are destroyed by step O3 as a component of the sequence generating process II. However, especially in a solution supersaturated with oxygen, the sequence (K0) + (L0) + (D1) + (H1) + (–Fi) becomes a link of a chain that regenerates the iodine atom that started it and produces the net chemical change of process III.

$$I_2 + 2HOOH \rightarrow HOI + HOIO + H_2O \quad (III)$$

Processes II and III as written involve formation of the stoichiometrically insignificant species HOIO, HOI, and I^-, and they also involve consumption of HOIO. Additional processes must be considered in order to describe net chemical change in terms of stoichiometrically significant species only. These additional processes will depend upon which steps from Table I are dominant in the system.

Hypoiodous acid, HOI, reacts mostly by the sequence (B0) + (A1) to generate the stoichiometry of process IV.

$$2HOI + HOOH \rightarrow I_2 + O_2(aq) + 2H_2O \quad (IV)$$

Formation of iodous acid, HOIO, from iodate, IO_3^-, can occur either by step A3 or B2. As pointed out above, step B2 is more important during the nonradical period when stoichiometry I is dominant. The relative importance of (B2) to HOIO formation will be even greater during the period of radical dominance when $[I^-]$ is less and the rate of (A3) is reduced while that of (B2) is relatively unaffected.

Consumption of HOIO is straightforward if it is being produced by process III more rapidly than it can be consumed directly either by process II or by reaction with the I^- produced in (II). Under these circumstances, second-order step A4 is the only process available to this excess iodous acid. Then the sequence (A4) + $^1/_2$(IV) = (A4) + $^1/_2$(A1) + $^1/_2$(B0) generates the stoichiometry of process V.

$$2HOIO + {}^1/_2HOOH \rightarrow IO_3^- + {}^1/_2I_2 + {}^1/_2O_2(aq) + H^+ + H_2O \quad (V)$$

We must also derive the stoichiometry of the consumption of iodide ion, I^-, produced in process II. This species reacts by the rapid equilibrium of step A1 and is formed and consumed at almost equal rates by steps –Fi and L0 during the chain sequence that generates process III. However, step A2 is the only one contributing much to net chemical change of iodide especially when dominance of radical processes has made step A3 unimportant. During dominance by nonradical processes, HOI is produced only by step A2 and the sequence (A2) + (IV) = (A2) + (A1) + (B0) generates the stoichiometry of process VI.

$$HOIO + I^- + HOOH + H^+ \rightarrow I_2 + O_2(aq) + 2H_2O \quad (VI)$$

However, when radical processes are also producing HOI by process III, the sequence (A2) + 2(A1) generates the stoichiometry of process VII. The validity of this analysis

$$HOIO + 3I^- + 3H^+ \rightarrow 2I_2 + 2H_2O \quad (VII)$$

is supported by Figure 7 which shows that steps A1 and A2 go at nearly the same net rate for long periods during which nonradical processes are dominant but that step A1 is about twice as fast as step A2 during the brief periods when radical processes are dominant.

These various stoichiometries can be combined to obtain the net chemical change resulting from the various radical processes. Let θ be the average chain length or the probability an iodine atom will initiate the chain sequence generating (III) divided by the probability it will undergo termination by step O3. Then the net chemical change due to radical processes generates the stoichiometry of (II) + 2θ(III). This stoichiometry can be combined with the other processes discussed above to generate net chemical change in terms of stoichiometrically significant species. The sequence (B2) + (II) + 2θ(III) + θ(IV) + $^2/_3$(VII) + ($\theta - {}^1/_3$)(V) generates the stoichiometry of process VIII.

$$({}^1/_2\theta - {}^1/_6)I_2 + ({}^{11}/_2\theta + {}^{29}/_6)HOOH \rightarrow (\theta - {}^1/_3)IO_3^- + ({}^3/_2\theta + {}^{17}/_6)O_2(aq) + (\theta - {}^1/_3)H^+ + (5\theta + 5)H_2O \quad (VIII)$$

This analysis of stoichiometry is more complete than that previously undertaken.[4,8] Nonradical processes reduce

iodate to iodine with a 5:1 ratio of O_2 to I_2 produced as shown with process I. If $\theta < 1/3$, radical processes also cause net reduction of iodate but simultaneously induce disproportionation of hydrogen peroxide. If $\theta > 1/3$, the net consequence of radical processes is the oxidation of iodine to iodate, but disproportionation of hydrogen peroxide is strongly induced at the same time. Oscillations are associated with alternating dominance by processes I and VIII.

Even a qualitative explanation of oscillations must consider changes in concentration of the three stoichiometrically insignificant species HOIO, HOI, and I^-. The following facts are relevant:

(a) The chain length θ increases with and is strongly dependent upon $[O_2](aq)$.

(b) Most of the oxygen is produced by step B0, and the rate of this step is proportional to [HOI].

(c) Rapid equilibrium A1 ensures that $[HOI][I^-] = [I_2]/K_{A1}[H^+]$. Therefore the *product* of these two concentrations is buffered by the slowly changing $[I_2]$.

(d) To a rough approximation, the rate of oxidation of I^- to HOI by steps A2 and A3 is equal to the rate of reduction of that species by step B0. Therefore

$$\frac{[I^-]}{[HOI]} \approx \frac{k_{B0}[HOOH]}{k_{A2}[H^+][HOIO] + k_{A3}[H^+]^2[IO_3^-]}$$

The *ratio* of the two key concentrations can change rapidly if and only if [HOIO] undergoes a major fractional change.

(e) The rate of process II is equal to that of step N2, and steps A2 and N2 both destroy HOIO at rates first order in that species.

(f) The rate of process III is 2θ times that of step N2. Therefore, if $(2\theta - 1)k_{N2}[IO_3^-] > k_{A2}[I^-]$, [HOIO] will increase rapidly and autocatalytically. If the reverse inequality becomes valid, [HOIO] will decrease rapidly.

The above facts permit us to describe an oscillatory cycle. Initially $[I_2]$ and $[O_2](aq)$ are both reasonably small and the system is in the nonradical period described by process I. In this situation, [HOIO] is relatively small, $[I^-] > [HOI]$, and $[I_2]$ is increasing slowly. As $[I_2]$ increases, the rate of process I also increases, $[O_2](aq)$ and θ increase, and a situation is ultimately reached such that $(2\theta - 1) \cdot k_{N2}[IO_3^-] > k_{A2}[I^-]$ and [HOIO] increases autocatalytically. Then $[I^-]/[HOI]$ decreases, and the increased [HOI] further increases the rate of oxygen production. The system switches to dominance by radical process VIII, and $[I_2]$ decreases while $[O_2](aq)$ continues high.

However, as $[I_2]$ decreases, [HOI] must eventually also decrease even though $[I^-]/[HOI]$ remains small. Then oxygen will be produced less rapidly, θ will decrease, and eventually $2(\theta - 1)k_{N2}[IO_3^-]$ will become less than $k_{A2}[I^-]$. Then HOIO will be destroyed more rapidly than it can be produced autocatalytically, $[O_2](aq)$ will fall precipitously, and the system will switch back to dominance by nonradical process I.

4. Thermodynamic Constraints

The rate constants in Table I are given for forward and reverse directions for each step and are intended to be consistent with thermodynamic constraints for the various species. The reasons for following such a procedure have been mentioned elsewhere.[10]

Assumed free energies of formation are presented in Table II. Standard state for H_2O is pure liquid; for every other species it is ideal 1 *m* solution. Most values have been taken from Latimer[11] as discussed previously and are based on measurements at 25 °C. The kinetic system being modeled reacted at 50 °C.

TABLE II: Free Energies of Formation of Aqueous Species (kcal/mol)

$H_2O(l)$	−56.690	IO_3^-	−32.250	$\cdot IO_2$	3.8
HOOH	−31.470	HOIO	−19.1	$\cdot OOI$	14.8
$HO\cdot$	8.53	HOI	−23.5	$\cdot IO$	25.3
$HOO\cdot$	3.0	I_2	3.926	$\cdot I$	16.12
O_2	4.136	I^-	12.35	H^+	0.000

Those free energies for which no experimental data exist were assigned as follows: The value for HOIO is based on regarding $\Delta G°$ for step A4 as analogous to data for chlorine and bromine chemistry.[4,8] The value for $\cdot IO_2$ was obtained in the same way with the use of halogen analogues of step N2.[4,8] The value for $\cdot I$ assumes the equilibrium constant for dissociation of I_2 in water is the same as in the gas phase; such a relation holds well in saturated hydrocarbons.[12,13] The value for $\cdot OOI$ is arbitrarily chosen so the concentration of this species will be ten times that of $\cdot I$ in a solution saturated with oxygen at 1 atm. The value of $\cdot IO$ makes this species appreciably more stable than was assumed previously;[4,8] otherwise step L0 would not have taken place at a sufficient rate if it had a conceivable reverse rate constant. The change is not seriously inconsistent with the chemistry of the other halogens.

The rate constant ratios from Table I were developed over a considerable period of trial computations, and they are not entirely consistent with the free energies in Table II. However, the internal consistency is within 4.6 kcal/mol for every step and is within 1.0 kcal/mol for every step whose reverse rate could be significant to the system modeled. We do not believe it is worth the effort to revise the rate constants to attain better internal consistency.

5. Assignment of Rate Constants

5.1. *General Considerations.* The mechanism from Table I contains 18 reversible steps whose rate constants must be assigned in such a way as to give net forward rates which reproduce experimental behavior as nearly as possible. Not all 18 pairs of rate constants are disposable parameters. Some are known independently from experiment, and some can be varied over wide ranges without significant effect on the behavior. The bases of assignment follow.

5.2. *Rate Constants from Experiment.* Rate constants for steps A1, A3, B0, B2, H1, and O1 are known with moderate confidence from experiment; the bases have been presented elsewhere.[4,8] The rate constant for (O3) was set equal to that in nonpolar solvents,[12] and k_{O2} was set equal to $2(k_{O1}k_{O3})^{1/2}$. This geometric mean assignment for the cross termination rate constant is a good approximation for many radical termination reactions, but it may not be valid for (O2) which is really an electron transfer reaction.

5.3. *Insensitive Rate Constants.* Step B1 need be included only to ensure the system will react even if no I^- is present initially, and the assignment will have little effect provided the assumed rate constant is not too large. The rate constants for (D1) and (D2) should be large enough that $\cdot IO$ and $\cdot IO_2$ radicals do not build up, but exact values are unimportant because the mechanism assigns no other fates to these species. Forward and reverse rate constants for step K0 should be large enough that the equilibrium is rapidly established, but the exact values are unimportant. The value of k_{-Fi} was chosen to be large enough that step O1 contributed to termination much less than step O3 did. Otherwise, the rate of reaction would be little affected by the concentration of dissolved oxygen.

5.4. *Initial Efforts to Assign Disposable Rate Constants.* The above assignments leave rate constants for the five steps A2, A4, L0, N2, and P as disposable pa-

rameters to be assigned so as to generate behavior observed in a typical experiment.

Our initial efforts treated step P as first order in the extent of supersaturation and assigned rate constants rather intuitively; the results were frustrating in the extreme. When k_{L0} was too small, $[I_2]$ increased to a stable steady state without any oscillations. When k_{L0} was too large, $[I_2]$ rose to a maximum and decreased while HOOH was destroyed by a single burst of radical reaction. In one set of computations, a factor of 2 change in k_{L0} and k_{-L0} went from a situation in which $[IO_3^-]$ scarcely changed to one in which it decreased precipitously by a factor of 10^{11} before it partially recovered! Oscillations remained conspicuous by their absence.

Past experience suggested the steady state would be less stable if k_P were made smaller, but then the hydrogen peroxide was consumed before dissolved oxygen reached a steady state. The first encouragement came from a calculation in which [HOOH] was maintained constant. This system did indeed go to an oscillatory state, but it oscillated about a steady state indicating oxygen saturation at about 100 atm or 1500 psi!

5.5. *Systematic Assignment of Rate Constants.* A more consistent procedure was finally adopted to assign the rate constants considered disposable. The system selected for modeling had initial concentrations $[IO_3^-]_0 = 0.1$ M, $[HOOH]_0 = 0.5$ M, $[H^+]_0 = 0.05$ M, $[O_2]_0 = [O_2]_{sat.} = 9.3 \times 10^{-4}$ M, and $[H_2O]_0 = 55$ M. Of course the concentration of water is virtually constant throughout, but the rate constants treat it as a reactant. The value of $[O_2]_{sat.}$ is the concentration at 50 °C of a solution saturated at 1 atm. Sometimes the model contained a small initial concentration of I^-, but this species need not be so included.

Our treatment regarded I_2 and O_2 as the only phase determining intermediates.[4,14] The objective was to select rate constants so the system would generate a steady state in which concentrations of these species are consistent with experiment. If the model is valid, this steady state should be unstable to oscillation.

The other nine species from Table II were assumed to be at negligible concentrations compared to the six mentioned above. Moreover $\cdot IO_2$, $\cdot IOO$, $\cdot IO$, and $HO\cdot$ were treated as what Clarke[15] calls flow-through reactants and were generally neglected. To treat other species, let us adopt the conventions $d[X]/dt = [\dot{X}]$ and ν_Y is the rate of step Y from left to right minus the rate from right to left. Seven equations can be written for the dynamic behavior of the phase determining and stiffly coupled intermediates.

$$[\dot{I}_2] = \tfrac{1}{2}\nu_{A3} + \tfrac{1}{2}\nu_{B2} - \tfrac{1}{2}\nu_{A4} - \tfrac{1}{2}\nu_{N2} = \nu_{A1} - \nu_{-Fi} + \nu_{O3} \quad (1)$$

$$[\dot{O}_2] = \nu_{B0} + \nu_{B2} + \nu_{-Fi} - \nu_{L0} - \nu_P \quad (2)$$

$$0 = \nu_{A3} + \nu_{B2} + \nu_{L0} - \nu_{A2} - 2\nu_{A4} - \nu_{N2} \quad (3)$$

$$0 = -\nu_{A2} - \tfrac{3}{2}\nu_{A3} + \tfrac{1}{2}\nu_{A4} + \nu_{B0} - \tfrac{1}{2}\nu_{B2} - \nu_{L0} + \tfrac{3}{2}\nu_{N2} - \nu_{O1} \quad (4)$$

$$[HOI] = [I_2]/(K_{A1}[H^+][I^-]) \quad (5)$$

$$\nu_{N2} = \nu_{O1} + \nu_{O2} + \nu_{O3} \quad (6)$$

$$0 = 2\nu_{N2} - 2\nu_{O1} - \nu_{O2} - \nu_{-Fi} + \nu_{L0} \quad (7)$$

The alternative expressions in eq 1 arise because $[\dot{I}_2] = -\tfrac{1}{2}[\dot{IO}_3^-]$. The $-\tfrac{1}{2}\nu_{N2}$ term is a substitution for $\tfrac{1}{2}\nu_{N2} - \tfrac{1}{2}\nu_{D2}$ because of the stoichiometric requirement that $\nu_{D2} = 2\nu_{N2}$.

Equation 2 neglects the contribution from step B1 as discussed above. To compute $[O_2]$ in terms of species not neglected, we can note that $\nu_{L0} = k_{L0}K_{K0}[H^+][\cdot I][I^-][O_2]$.

Equation 3 says $[\dot{HOIO}] = 0$; it again neglects the contribution from step B1.

Equation 4 says $[\dot{I}^-] = 0$. Because ν_{A1} is a small difference between two large numbers, it has been eliminated by use of the two expressions from eq 1. Equation 4 as written here also includes a substitution from eq 6.

Equation 5 assumes step A1 is in rapid equilibrium.

Equation 6 says rates of formation and destruction of radical species are equal.

Equation 7 says $[\dot{HOO}\cdot] = 0$.

It is useful to use the designation n to refer to a hypothetical nonradical situation in which no radical processes are significant and in which state of solution of oxygen is ignored. The only steps of importance in such a situation would be (A1), (A2), (A3), (B0), and (B2), and the stoichiometry of net chemical change would be $2IO_3^- + 5HOOH + 2H^+ \rightarrow I_2 + 5O_2 + 6H_2O$. Then

$$[HOIO]_n = \frac{\nu_{A3}(n) + \nu_{B2}(n)}{k_{A2}[H^+][I^-]_n} \quad (8)$$

$$2\nu_{B0}(n) = 5\nu_{A3}(n) + 3\nu_{B2}(n) \quad (9)$$

We arbitrarily assigned k_{A2} expecting it to be large because of the analogy with the oxybromine system and could then use eq 5, 8, and 9 to calculate $[HOIO]_n$ given any value of $[I_2]$. At all times, $[HOIO] \geq [HOIO]_n$.

The above procedures leave all rate constants assigned except those for steps A4, L0, N2, and P. These are calculable with the use of four additional constraints assumed to apply to the steady state:

$$[I_2]_{ss} = 0.001 \text{ M} \quad (10)$$

$$[O_2]_{ss} = m[O_2]_{sat.} \quad (11)$$

$$[HOIO]_{ss} = 30[HOIO]_n \quad (12)$$

$$\nu_{N2}(ss) = \nu_{A4}(ss) \quad (13)$$

Equation 10 is chosen to be consistent with experimental observations.

Equation 11 leaves the parameter m for subsequent assignment as discussed below. It must obviously be greater than or equal to unity.

The factor 30 in eq 12 assumes the ratio of maximum (pure radical) and minimun (pure nonradical) concentrations of HOIO is about 1000 and the steady state generates approximately the geometric mean. We previously[4,8] argued on the basis of $[I^-]$ ranges that the ratio of the [HOIO] extremes was 100 but increased the range in the calculations in an initially unsuccessful attempt to make the model more sensitive to oscillation. In the Belousov–Zhabotinsky reaction,[6,7] the limiting concentrations of HOBrO differ by a factor of about 10^5.

Finally, eq 13 is based on an analogy to the Oregonator[16] model predicting the system will be most sensitive to oscillation if the first-order rates of formation and consumption of HOIO are equal at the steady state. Let θ be the ratio of the rate at which HOIO is created by step D1 divided by the rate at which $\cdot IO_2$ radicals are formed by step N2; this ratio is analogous to a chain length and may in principle have any positive value. If the system is in a steady state, the rate at which lower oxidation states are oxidized to HOIO is equal to the rate at which HOIO is reduced; then $2\theta\nu_{N2} = \nu_{A2} + \nu_{A4}$. The equality of rates of first-order formation and destruction of HOIO leads to $(2\theta - 1)\nu_{N2} = \nu_{A2}$. Equation 13 follows directly.

These relations permit all rate constants to be assigned on the basis of the single parameter m which is to be selected to make the steady state unstable to oscillation.

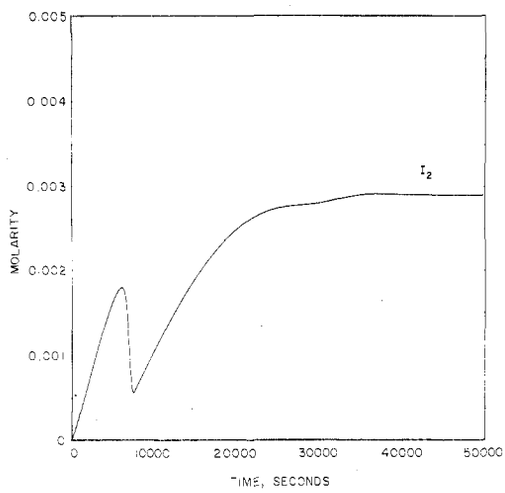

Figure 1. Calculated behavior of I_2 with time, closed system model, $[HOOH]_0 = 0.5$ M.

The value selected for m affects the rate constants selected for steps L0 and P only.

5.6. *Determination of Steady State Stability.* As we[14] and several others have pointed out, the steady state in a system with only two phase determining intermediates cannot be oscillatory unless

$$(\partial[\dot{I}_2]/\partial[I_2])_{[O_2]} + (\partial[\dot{O}_2]/\partial[O_2])_{[I_2]} > 0 \qquad (14)$$

For the system being modeled, we found

$$\partial[\dot{I}_2]/\partial[I_2] = 1.49 \times 10^{-5}\ s^{-1} \qquad (15)$$

$$\partial[\dot{O}_2]/\partial[O_2] = r/m - s/(m-1) \qquad (16)$$

where r and s are positive quantities with s and s alone depending upon the kinetics assumed for step P. We can see that if m is sufficiently close to unity, the expression in eq 14 will be negative and the steady state will be stable and nonoscillatory. If m is sufficiently large, the expression will be positive and the system will oscillate. The problem is to select a proper value of m.

6. Results

6.1. *Linear Supersaturation Kinetics.* Our initial modeling efforts were all made with the assumption that relief of supersaturation was a first-order process and

$$v_P = k_a\{[O_2] - [O_2]_{sat.}\} \qquad (17)$$

For the assignments discussed above, $v_P(ss) = 2.17 \times 10^{-5}$ M s^{-1} and $k_a = 0.0233/(m-1)\ s^{-1}$.

Only later did we discover that these kinetics apparently require that $r < s$ in eq 16. For these kinetics, oscillations will only be possible when m is so large that eq 15 is greater than the magnitude of eq 16. Such a result required an m of the order of 100. Our modeling efforts based on eq 17 were necessarily doomed to failure.

6.2. *Fourth Root Supersaturation Kinetics.* We then arbitrarily changed the kinetics of step P to become

$$v_P = k_b\{[O_2] - [O_2]_{sat.}\}^{1/4} \qquad (18)$$

The rate of degassing is thus made less sensitive to changing oxygen concentration. When these kinetics were applied to the conditions discussed above, we calculated $k_b = 1.24 \times 10^{-4}/(m-1)^{1/4}$ $M^{3/4}$ s^{-1}, $r = 0.0174\ s^{-1}$, $s = 0.00582\ s^{-1}$ with the steady state unstable to oscillation whenever $m > 1.50$.

Figure 1 shows changes in $[I_2]$ on a linear scale for such a system with $m = 2$. A few maxima and minima really do occur, but the system is a poor approximation to the experimental observations shown in Figure 2. Oscillations in the model system die out because hydrogen peroxide is rapidly consumed whenever the radical processes become dominant.

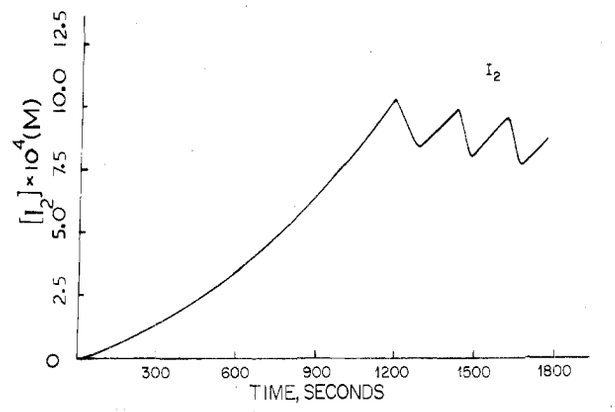

Figure 2. Observed closed system behavior of I_2 with time, $[HOOH]_0 = 0.49$ M, $[IO_3^-]_0 = 0.104$ M, $[H^+]_0 = 0.047$ M. (Reprinted from ref 4.)

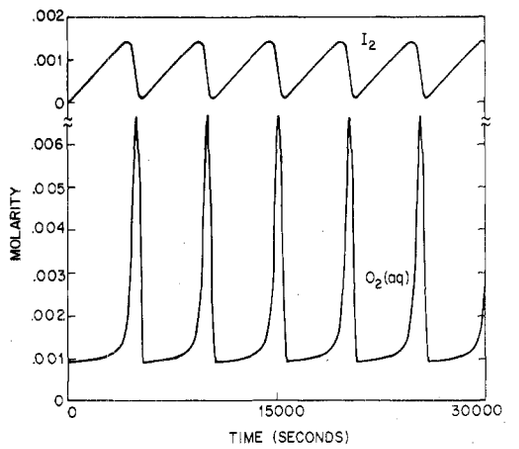

Figure 3. Calculated behavior of dissolved O_2 (lower curve) and I_2 with time, constant HOOH model. Initial conditions were as follows: $[IO_3^-]_0 = 0.1$ M, $[HOOH]_0 = 0.5$ M, $[H^+]_0 = 0.05$ M, $[O_2]_0$(aq) $= 9.3 \times 10^{-4}$ M (saturation concentration); $m = 2$.

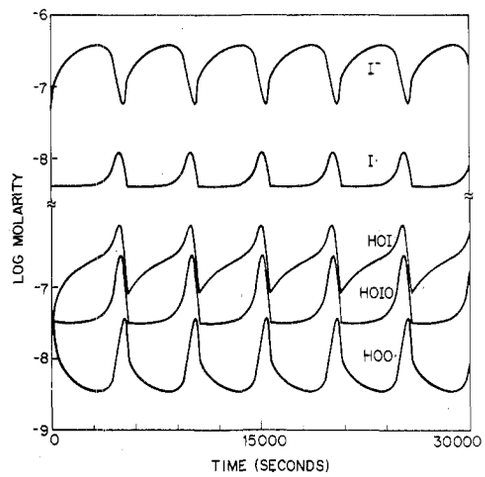

Figure 4. Calculated behavior of (top to bottom) I^-, ·I, HOI, HOIO, and HOO· with time, constant HOOH model. Conditions of Figure 3.

6.3. *Behavior at Constant [HOOH].* We then altered the program to maintain [HOOH] constant at 0.5 M instead of allowing this species to be depleted. The calculations now generated magnificent sustained oscillations. Figures 3 and 4 show the calculated behavior of $[I_2]$, $[O_2]$, $[I^-]$, [HOI], [·I], and [HOO·]. Comparative closed system experimental behavior of $[I_2]$, $[O_2]$, and $[I^-]$ is shown in Figures 2 and 5.

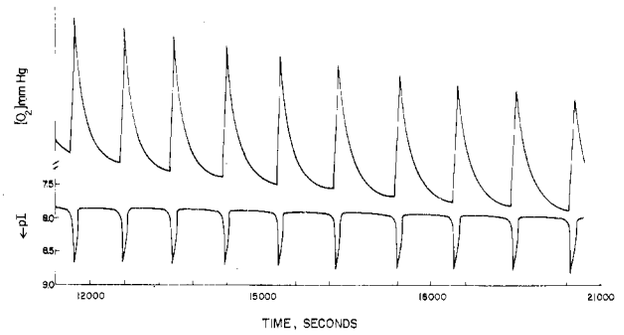

Figure 5. Observed behavior of dissolved O_2 (upper trace) and I^- with time. $[HOOH]_0 = 0.098$ M, $[IO_3^-]_0 = 0.105$ M, and $[H^+]_0 = 0.059$ M. (Reprinted from ref 3.)

The calculations at constant hydrogen peroxide concentration correspond encouragingly well with the experimental observations. However, the concentration of dissolved oxygen rises to the equivalent of saturation at more than 5 atm even though the (unstable) steady state corresponds to only about 2 atm. The experimental observations in Figure 5 correspond to a range of oscillating oxygen concentrations equivalent to only about a 0.5 atm change in saturation pressure. The kinetics of eq 18 evidently slow the computed response to increasing $[O_2]$ so that oxygen promoted radical decomposition of hydrogen peroxide is not easily shut off even after $[I_2]$ has been driven to low levels. Ways to correct for this modeling failure are discussed below.

6.4. *Effect of Acidity on Behavior.* One of the more remarkable features of the Bray–Liebhafsky reaction is the great dependence of behavior on acid concentration.[4,8] If $[H^+]$ is less than about 0.04 M, $[I_2]$ increases smoothly until the element precipitates before an oscillatory steady state is attained. If $[H^+]$ is between about 0.04 and 0.055 M, the system oscillates after an induction period; the lower the acidity the larger the amplitude of oscillations and the greater the sensitivity to external influences such as light, stirring, etc. If $[H^+]$ is between about 0.055 and 0.06 M, $[I_2]$ rises to a rounded maximum and then decreases during a second induction period before small amplitude oscillations finally commence. If $[H^+]$ is above about 0.06 M, $[I_2]$ decreases smoothly after its maximum and hydrogen peroxide undergoes a catalyzed decomposition such that $[I_2]/[HOOH]$ remains a nearly constant ratio.

Effects of changing acidity provide a severe test for the validity of our model mechanism. Figure 6 shows a series of computations in which [HOOH] was maintained constant at all times at 0.5 M while $[H^+]_0$ was varied between 0.02 and 0.2 M. The computations show that $[I_2]$ is greater at lower acidity and that the amplitude of any oscillations is also larger at lower acidity. The computations generate oscillations over a somewhat wider range of acidity than is observed experimentally, but the qualitative effects are in good agreement with experiment.

6.5. *Effect of Hydrogen Peroxide Concentration on Behavior.* As was mentioned above, when $[H^+]$ is between 0.055 and 0.06 M the experimental system exhibits a second induction period during which $[I_2]$ decreases smoothly before oscillations finally commence. Hydrogen peroxide is decreasing during this second induction period, and it appears that at moderately great acidities there is a maximum [HOOH] above which the steady state is nonoscillatory. We attempted to test this interpretation by a series of computations in which [HOOH] was maintained constant at different values. We did indeed find maximum and minimum hydrogen peroxide concentrations beyond which oscillations did not occur.

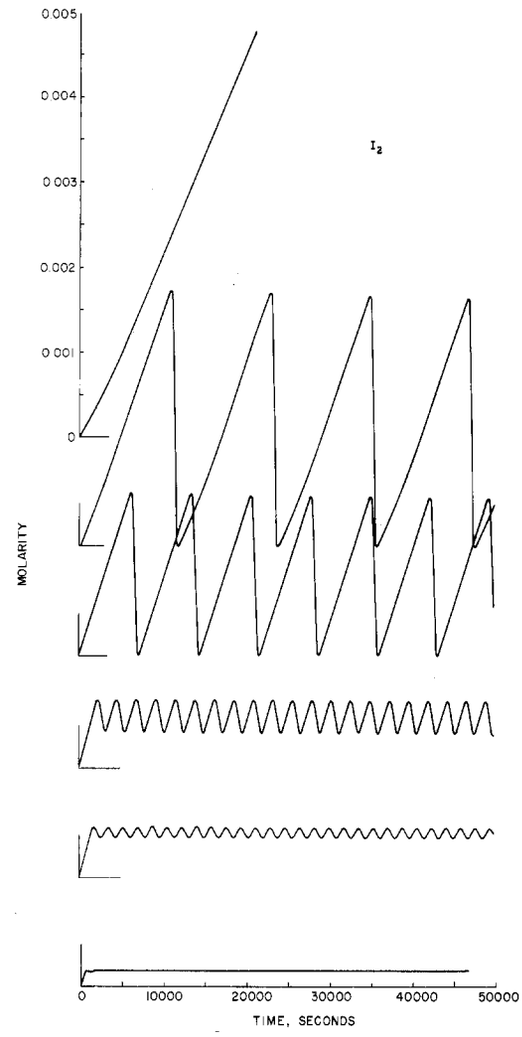

Figure 6. Calculated behavior of I_2 with time, constant HOOH model. [HOOH] = 0.5 M. $[H^+]_0$ = (top to bottom) 0.02, 0.03, 0.04, 0.08, 0.1, 0.2.

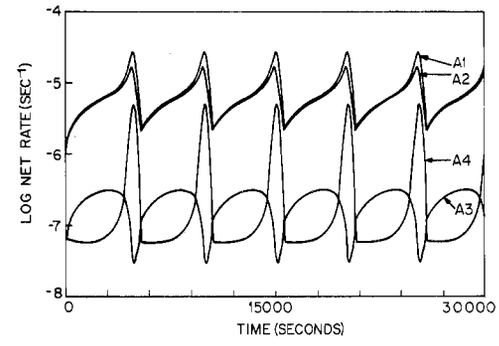

Figure 7. Calculated net rates of (A) steps. Conditions of Figure 3.

However, computed iodine concentrations varied *inversely* with hydrogen peroxide whereas experimental observations[2,4] indicate $[I_2]$ and [HOOH] are *directly proportional* during the second induction period. We can rationalize the discrepancy by the fact that our model selected rate constants so that at 0.5 M hydrogen peroxide the steady state supersaturation corresponded to $m \doteq 2$. The computations at other concentrations gave completely unrealistic concentrations of dissolved oxygen, and we believe our problems involved our model for release of supersaturation rather than that for chemical mechanism.

6.6. *Rates of Individual Steps.* Experimental measurements are usually confined to concentrations of individual species. However, computations can also generate rates of individual steps, and those rates often provide

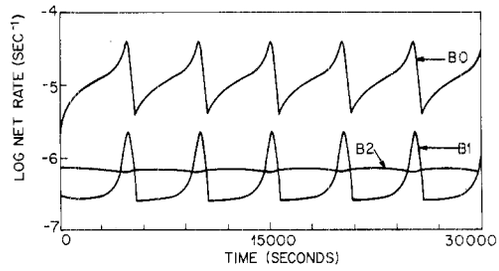

Figure 8. Calculated net rates of (B) steps. Conditions of Figure 3.

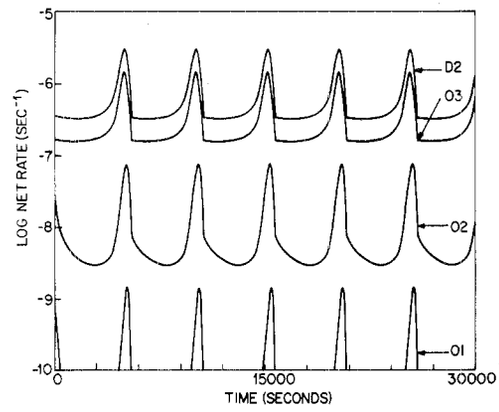

Figure 9. Calculated net rates of step D2 and O steps. Step N2 is almost coincident with step O3. Conditions of Figure 3.

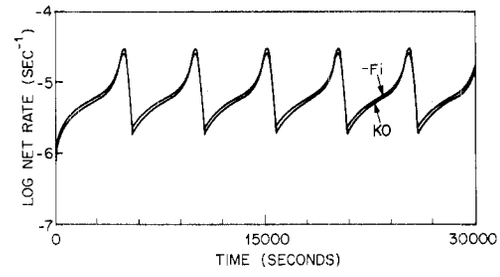

Figure 10. Calculated net rates of steps K0, lower curve, and –Fi. Steps D1 and L0 are coincident with step K0. Conditions of Figure 3.

additional insights. Figures 7–10 show such rates for the same conditions used to compute concentrations in Figures 3 and 4.

The results strongly support the argument of section 3. Thus radical initiation and termination steps N2 and O3 always go at almost identical rates while step D2 is always twice as fast. The rates of steps K0, L0, and D1 are almost superimposable, while the rates of steps H1 and –Fi are only slightly greater with the greatest difference occurring when θ is smallest at the start of the nonradical period. As pointed out earlier, steps A1 and A2 go at almost identical rates when process VI can best describe the reaction of I^- with HOI, but step A1 becomes twice as fast as step A2 when process VII becomes the better description.

These detailed consistencies serve to support the general validity of the often involved arguments by which the model mechanism was developed.

7. Discussion

As was indicated in the Introduction, this study was undertaken in the expectation the Bray–Liebhafsky reaction would be easier to model than the complicated organic chemistry of the Belousov–Zhabotinsky reaction.[6,7] Instead, we found the modeling of release of dissolved gas introduced complications at least as severe.

If the rate of oxygen escape is assumed proportional to the degree of supersaturation, as in eq 17, the system is too sensitive to changes in concentration of dissolved oxygen. It took us 1 year of frustration before we realized oscillations would only be possible at oxygen concentrations so great that all of the initial hydrogen peroxide would be destroyed long before the necessary conditions were attained.

If the rate of oxygen escape is assumed much less sensitive to the degree of supersaturation as in eq 18, an unstable steady state is attained at a plausible concentration. However, that steady state is overshot so far that decomposition of most of the hydrogen peroxide is induced during a very small number of oscillations. Only by the computational device of constantly replenishing the hydrogen peroxide were we successful in modeling the behavior observed experimentally in closed systems.

We doubt that experimental behavior in closed systems could be modeled by modifying eq 17 and 18 to develop other kinetics for step P as a continuous function of degree of supersaturation. We were successful, however, if we tried to simulate the nucleation of bubbles. Insensitive kinetics such as eq 18 would apply until the concentration of dissolved oxygen had risen somewhat above the steady state and radical process V had become dominant. The computation then switched discontinuously to a much larger rate constant for rapid release of supersaturation by process P, and this constant would continue until $[O_2]$ had fallen to near saturation. The kinetics would then return to eq 18. Such a model is inherently plausible and was made to generate oscillations. Critics could justifiably complain that such ad hoc procedures relied too heavily on methods first developed by Procrustes.[17] It is amply clear, however, that a successful model would have to deal correctly with this factor, which is an area of extreme complexity and considerable uncertainty at the present time.[18]

We must admit failure to model closed system behavior well, and at the present time the directions for continued efforts are unclear. However, we also believe our present level of success is impressive for a system as complicated as this one. All of the species in Table II are either well known or are analogous to known species and have bonds consistent with current theories of valence. The 17 steps other than (P) are all elementary processes and either are known from studies in other systems or are analogous to known reactions. Rate constants for all except 4 of those 17 steps either are known from independent experimental measurement or else can be varied over a wide range without significant influence on behavior. A self-consistent set of thermodynamic assignments and inclusion of all reverse rate constants has ensured we did not fall into any traps involving microscopic reversibility.[10] We have introduced the single additional feature of constantly replenishing the hydrogen peroxide as it is consumed, and we have then semiquantitatively reproduced several unusual features such as the oscillations themselves and the effects of changing acidity.

Of course no chemical mechanism is ever "proved" with absolute certainty, but it seems unlikely a markedly different mechanism can be devised that is as consistent with valence theory, thermodynamics, and known kinetics and that reproduces equally well the remarkable experimental features of this reaction. We believe we can fairly claim to understand the essential features of the mechanism.

References and Notes

(1) W. C. Bray, *J. Am. Chem. Soc.*, **43**, 1262 (1921).
(2) The latest paper in a long series is H. A. Liebhafsky, W. C. McGavock, R. J. Reyes, G. M. Roe, and L. S. Wu, *J. Am. Chem. Soc.*, **100**, 87 (1978).

(3) K. R. Sharma and R. M. Noyes, *J. Am. Chem. Soc.*, **97**, 202 (1975).
(4) K. R. Sharma and R. M. Noyes, *J. Am. Chem. Soc.*, **98**, 4345 (1976).
(5) B. L. Clarke, private communication.
(6) D. Edelson, R. J. Field, and R. M. Noyes, *Int. J. Chem. Kinet.*, **5**, 417 (1975).
(7) D. Edelson, R. M. Noyes, and R. J. Field, *Int. J. Chem. Kinet.*, in press.
(8) Supplemental materials from ref 4.
(9) R. M. Noyes and R. J. Field, *Acc. Chem. Res.*, **10**, 273 (1977).
(10) R. M. Noyes, *J. Phys. Chem.*, **81**, 2315 (1977).
(11) W. M. Latimer, "Oxidation Potentials", 2nd ed, Prentice-Hall, New York, 1952.
(12) J. Zimmerman and R. M. Noyes, *J. Chem. Phys.*, **18**, 658 (1950).
(13) M. Gazith and R. M. Noyes, *J. Am. Chem. Soc.*, **77**, 6091 (1955).
(14) R. J. Field and R. M. Noyes, *Acc. Chem. Res.*, **10**, 214 (1977).
(15) B. L. Clarke, *J. Chem. Phys.*, **64**, 4165 (1976).
(16) R. J. Field and R. M. Noyes, *J. Chem. Phys.*, **60**, 1877 (1974).
(17) "Encyclopedia Britannica" Vol. 18, 1970, p 587.
(18) A. C. Zettlemoyer, "Nucleation", Marcel Dekker, New York, 1969.

Radiation Chemistry of Aqueous Solutions of Dicyandiamide

Z. D. Draganić,* I. G. Draganić, and K. Sehested†

Boris Kidrič Institute of Nuclear Sciences, Beograd 11001, Yugoslavia *(Received March 2, 1978)*

Oxygen-free aqueous solutions of dicyandiamide, DCDA, were exposed to ^{60}Co γ rays or a pulsed 10-MeV electron beam. Fast kinetic spectrophotometry was used for the study of free-radical intermediates, and computer simulation of the reaction mechanism for evaluation of experimental data. The hydrated electron reacts by addition, $k(e_{aq}^- + DCDA) = 1.1 \times 10^{10}$ M^{-1} s^{-1}; the anion radical $[NH_2C(=NH)NHCN]^-$ absorbs in the UV region with λ_{max} <255 nm and an $\epsilon(255)$ of 1150 M^{-1} cm^{-1}. It disappears with $2k = 1 \times 10^9$ M^{-1} s^{-1} by forming a product which absorbs with λ_{max} <255 nm and an $\epsilon(255)$ of 2400 M^{-1} cm^{-1}. The hydrogen atom also reacts by addition, $k(H + DCDA) = 2.7 \times 10^6$ M^{-1} s^{-1}, and the radical intermediate has a λ_{max} of 350 nm and an $\epsilon(350)$ of 1250 M^{-1} cm^{-1}; it disappears with $2k \geq 10^9$ M^{-1} s^{-1}. Hydroxyl radicals react both by addition and by abstraction, $k(OH + DCDA) = 5.6 \times 10^6$ M^{-1} s^{-1}, and two transients with λ_{max} at 450 and 355 nm appear. It is estimated that about 90% of OH radicals react by abstraction. It has also been found that the radical-anion $SO_4^{-\cdot}$ reacts efficiently with DCDA and the product of this reaction, $NH_2^+C(=O)NHCN$, absorbs light with a λ_{max} of 355 nm and $\epsilon(355)$ of 1150 M^{-1} cm^{-1}. The OH adduct of DCDA has a λ_{max} of 450 nm and $\epsilon(450)$ of 1700 M^{-1} cm^{-1}; it disappears by a second-order process with $2k \leq 4 \times 10^9$ M^{-1} s^{-1}. The search for stable radiolytic products in the kilorad–megarad dose range has shown the presence of only a few smaller molecules and in low yields.

Introduction

The action of ionizing radiations on simple RCN molecules leads to various chemical changes in aqueous media which are of interest to the studies of prebiotic chemical evolution.[1-3] There are no published data on the radiation chemistry of dicyandiamide (DCDA), i.e., the dimer of NH_2CN. The molecule, $NH_2C(=NH)NHCN$, which can easily be produced by laboratory experiments simulating primitive earth conditions,[4] is considered as a compound that might have had a significant role in prebiotic molecular evolution.[5] The present work reports on the early stages of radiation-induced chemical process in oxygen-free aqueous solutions of DCDA, as well as on the compound identified in samples irradiated by kilorad–megarad doses. Computer calculations were used to determine concentrations of intermediates and to derive rate constants which could not be obtained directly from experiments.

Experimental Section

Chemicals. DCDA was BDH Laboratory Reagent Grade (mp 209–212 °C) minimum assay 99%, sulfated ash not more than 0.05% and was used without further purification. Other chemicals used for reagents preparations were the best purity research grade commercially available.

Analyses. Various techniques used in this work are given in full detail elsewhere.[3,6] Special attention was paid to the blank correction in CO_2 measurements; $HClO_4$ was added to adjust the pH to about 5 and minimize the blanks. Spectrophotometric determination of the DCDA concentration was made with a mixture of 1% aqueous solutions of $Na_2[Fe(CN)_5(CO)]$, $K_3[Fe(CN)]_6$, and NaOH as the reagent.[7] The molar extinction coefficient of the colored complex was 640 M^{-1} cm^{-1} at λ_{max} 510 nm. A Durum 500 amino acid analyzer in the Laboratory of Chemical Evolution (Chemistry Department, University of Maryland) was used for amino acid assays.

Irradiations. The radioactive cobalt source at Vinča was used for steady-state experiments; the dose rates varied between 1.5 and 35 krd min^{-1}. Pulsed beam experiments were performed at Risö National Laboratory (Risö, Denmark) by using a 10-MeV electron accelerator and the setup for fast kinetic studies described elsewhere.[8] Irradiation of the samples was performed at room temperature; heating of the solutions during irradiations was not significant at the dose rates used.

Computer simulation was used to compute the concentrations of short-lived intermediates and to determine some rate constants that could not be measured directly. The computations were made on a Burroughs 6700 computer at Risö.[6]

The following reactions of primary radicals in irradiated pure water were considered in the reaction model:

$$e_{aq}^- + H_3O^+ \rightarrow H + H_2O \qquad k_1 = 2.1 \times 10^{10}\ M^{-1}\ s^{-1} \quad (1)$$

$$e_{aq}^- + OH \rightarrow OH^- \qquad k_2 = 3 \times 10^{10}\ M^{-1}\ s^{-1} \quad (2)$$

$$e_{aq}^- + H \xrightarrow{H_2O} H_2 + OH^- \qquad k_3 = 2.5 \times 10^{10}\ M^{-1}\ s^{-1} \quad (3)$$

† Accelerator Department, Risö National Laboratory, DK 4000 Roskilde, Denmark.

0022-3654/79/2083-0220$01.00/0